Cleaner Materials 4 (2022) 100073

Contents lists available at ScienceDirect

Cleaner Materials

journal homepage: www.elsevier.com/locate/clema

Investigation of the influence of Off-Spec coal combustion waste on asphalt binder rheological performance and aging sensitivity

Ahmed Abdalla [a,*], Ahmed F. Faheem [a], Mohammed Alsalihi [b], Konstantin Sobolev [c]

[a] Department of Civil and Environmental Engineering, College of Engineering, Temple University, 1947 N 12th St, Philadelphia, PA 19122, United States
[b] Bureau of Construction Services and Materials, New Jersey Department of Transportation, 1 Executive Campus, Cherry Hill, NJ 08002, United States
[c] Department of Civil and Environmental Engineering, College of Engineering, University of Wisconsin-Milwaukee, 3200 N Cramer St, Milwaukee, WI 53211, United States

ARTICLE INFO

Keywords:
Upcycling
Off-spec Fly Ash (OFA)
Asphalt aging
Asphalt healing
FTIR
Physio-chemical
Coal combustion wastes (CCW)

ABSTRACT

Previous studies show promising effects of some standard fly ash classes on asphalt. However, there is limited research into off-spec fly ash. Multiple studies published presented fly ash as unique compared to traditional mineral fillers. In this paper, several coal combustion wastes (CCW) are examined in terms of their physio-chemical interaction with asphalt binders. Eight types of CCW are blended with two types of asphalt binders: unmodified and polymer modified (PMA). The physical properties and chemical composition of the CCW are characterized. Testing is focused on identifying changes in binder performance after blending with the CCW to understand the role of the CCW. The experimental program is focused on damage healing, rheological performance, and Low-temperature cracking potential. All the blends are conditioned using the pressure aging vessel. Oxidative aging is quantified through measurement of both carbonyl (ICO) and sulfoxide (ISO) indices by Fourier-Transform Infrared Spectroscopy (FTIR). Results show that some of the CCWs are associated with improved rheological performance, damage healing, and cracking resistance. The improvement is attributed to the level of interaction between the binder and the CCW and the physical and chemical characteristics of the CCW. Testing results demonstrate that synergy between the CCW particles and polymer modifiers needs further investigation. Statistical regression analysis is used to quantify the level of significance of influencing factors on the blend performance. The analysis revealed that the level of interaction between the CCW and the binder is measurable by the phase angle of the blend. The CCW's silicon (Si), Sulfur (S) content, along with particle size distribution and specific gravity, are the significant chemical and physical properties influencing the blend performance. These findings propose a fruitful upcycling opportunity for some CCW as an enhancer of asphalt performance.

Contents

Introduction . . . 2
Materials and methods . . . 3
- Materials . . . 3
- CCW chemical and physical testing . . . 3
- Laboratory testing methods to evaluate binder blends . . . 3
- Chemical analysis using FTIR . . . 4
- Rheological time and temperature dependency . . . 4
- Damage behavior . . . 4
- Damage healing characterization . . . 5
- Low-Temperature cracking susceptibility using bending beam rheometer BBR . . . 5
- Experimental design . . . 5
- Fabrication of blends . . . 5
- Testing results and discussion . . . 6

* Corresponding author.
E-mail addresses: tuh37876@temple.edu (A. Abdalla), afaheem@temple.edu (A.F. Faheem), mohammed.alsalihi@dot.nj.gov (M. Alsalihi), sobolev@uwm.edu (K. Sobolev).

https://doi.org/10.1016/j.clema.2022.100073
Received 15 October 2021; Revised 28 February 2022; Accepted 26 March 2022

Testing results and discussion . . . 7
Chemical and physical characterization of fly ash . . . 7
CCW chemical composition . . . 7
Particle shape and size distribution of fly ash . . . 7
Fractional voids (Rigden Voids) . . . 7
Asphalt blends performance . . . 8
Superpave performance grading results . . . 8
Analysis of infrared spectroscopy (FTIR) . . . 10
Damage healing evaluation . . . 10
Fly ash Physio-chemical influence on asphalt binder's healing performance . . . 11
Crossover modulus (G_c*) . . . 12
Fly ash Physio-chemical influence on asphalt binder's aging indicator (G_c*) . . . 12
Low-Temperature performance evaluation . . . 13
Fly ash Physio-chemical influence on asphalt binder's Low-Temperature performance (ΔT_c) . . . 13
Recommended future work . . . 13
Conclusion . . . 13
Declaration of Competing Interest . . . 14
Acknowledgment . . . 14
References . . . 14

Introduction

Coal combustion Waste (CCW) is a viable source for recycling due to the large quantities produced yearly in the United States. According to the American Coal Ash Association (ACAA), 41% of produced CCW is disposed of in landfills in 2020, constituting more than 28.4 million tons (ACAA, 2020). For many years fly ash has been effectively used as a partial replacement for Portland cement in producing different types of concrete, embankments, and soil stabilization. Fly ash is rarely used in flexible pavement construction. However, lately, there has been renewed interest in employing it as a mix design component (Sobolev et al., 2014, Bautista, 2015, Li and Yang 2021, Muhammad et al., 2021). However, the focus of this recent interest is directed mainly to standard fly ash classes. These classes of fly ash are already utilized at a steadily increasing rate, according to the ACAA. On the other hand, other CCWs are underutilized at an alarmingly high rate. Material like flue gas desulfurization scrubber has < 5% utilization (ACAA, 2020). Most of the underutilized materials are formed when coal-burning power plants burn coal at low temperatures to minimize their CO_2 and SO_2 emissions. Therefore, these types of CCW are referred to as Off-spec Fly Ash (OFA). They may have a high carbon and sulfur contents, hindering off-spec ash use with cementitious materials.

In the literature related to the interaction of particulates with the asphalt binder, papers have been published since the early 1900s. Many of these studies labeled these particulates as fillers. Typically, fly ash is treated as a filler in most studies. However, in a study sponsored by the National Cooperative Highway Research Program (NCHRP), the researchers suggested that fly ash's influence on the binder does not match that of the mineral fillers (Faheem et al., 2010). The researchers of the study followed up with additional experimentations to evaluate the interaction between fillers and asphalt binders, including fly ash. In this study, particulates (mineral fillers and fly ash) were incorporated with the binders at different volume concentrations. Testing evaluated the stiffness change and tack strength of the mastics. The results confirmed the observation of the NCHRP study, where the fly ash interaction with binders was unique. Later, two studies evaluated mixture compaction and performance by replacing 10% of the binder with fly ash while keeping the aggregate structure (gradation) constant. The first study by Faheem et al. in 2017 used three types of fly ash, including one off-spec ash. The results showed that using 10% fly by weight of the asphalt binder did not change the compaction effort required to achieve density targets. The laboratory performance testing of the mixtures focused on testing moisture damage resistance, fatigue life, and thermal cracking. The reported results show a significant increase in fatigue life measured as the number of cycles to 50% drop of the complex dynamic modulus. The moisture damage tensile strength ratio (TSR) following the AASHTP T283 procedure indicated no change in the TSR even with the lower asphalt binder content. Mixture thermal cracking tested using the semi-circular bending geometry resulted in a significant fracture energy increase at −18 °C. In addition, the ash containing mixes exhibited lower stiffness at this temperature compared to the control mixes (containing 10% more binder). The research team repeated similar work for off-spec ash with warm mix asphalt (Cloutier et al., 2017a, Cloutier et al., 2017b). The published results follow the exact same trend. These results raise the suggestion that fly ash may be interacting with the binder as an additive rather than a filler.

Few studies evaluated this hypothesis regarding fly ash as an additive. Bautista et al. (2015) investigated the rheological performance of asphalt binders with different types of CCWs in terms of correlation with fly ash's chemical and physical properties. Faheem et al. (2017) validated that some CCWs can work as enhancers and extenders to the binder. The authors also demonstrated that some CCW products could enhance the mixture of aging resistance, moisture damage resistance, fatigue life, and thermal cracking resistance. In *2017,* Saha *et al.* investigated the structure of asphalt blends with fly additives using atomic force microscopy. They reported that the addition of fly ash could increase the area of the micelle structures and correlated the area to the complex modulus of blends Saha et al. (2017).

Nevertheless, this research's novelty comes as there is a lack of research evaluating the fly ash- asphalt physio-chemical interaction. This could be influenced by the difficulty of quantifying such interaction or due to the complex nature of the asphalt binders (Clopotel et al., 2012). However, there were decent efforts made by many researchers studying asphalt-filler interactions, but not fly ash-asphalt physio-chemical interaction *(*Faheem et al., 2011; Liu et al., 2018; Zhang et al., 2019; Guo and Tan, 2021*)*.

Recently, two studies have been published focusing on the physicochemical interaction of fly ash and asphalt. Li and Yang, in a paper, published 2021, evaluated morphological and chemical characteristics of asphalt blended with limestone and fly ash particulates at 50%

dosage by mass. The authors clearly indicate that fly ash is not an inert filler. The authors concluded that the physicochemical interaction of the fly ash and asphalt blends resulted in better aging resistance performance than limestone and asphalt blends (Li and Yang, 2021). Muhammad et al. (2021) conducted a comprehensive study on asphalt mixtures containing fly ash and bone glue. The authors claimed that the fly ash and bone glue modified the asphalt binder. The testing results showed that the fatigue life measured by the four-point-bending beam fatigue test is 89.5% higher when the binder is replaced with 10% bone glue and 6% fly ash. These two recent studies are among the very few research treating fly ash as an additive rather than a filler.

Given the above discussion, this paper aims to investigate the interaction between asphalt binder and different CCWs. The main hypothesis is that some of the CCWs act as additives. The following objectives are selected to test this hypothesis:

Investigate the chemical and physical properties of various OFA sources and evaluate their physio-chemical influence on the aging and healing capability of binder and ash blends.
Quantify change in the chemical composition of the blend of OFA and binder under simulated aging.
Quantify damage performance of the blend under the viscoelastic regime and elastic regime.
Highlight the rheological profile of the blends.

No rejected this study's objective could result in establishing a new market for some CCWs as upcycled additives.

Materials and methods

Materials

Two binders are selected in this study; a neat PG 64–22 binder and a Styrene-Butadiene-Styrene (SBS) Polymer Modified Asphalt (PMA) binder PG 76–22. Eight types of CCW are mixed with the two types of binders at 10% by weight. This dosage is selected to be in accordance with previously published studies (Bautista et al., 2015; Cloutier et al., 2017a, Cloutier et al., 2017b; Faheem et al., 2017). The eight types of fly ash were obtained from eight different electric power plants in six different states. GA, BH, SBH, RH, WE, RO, HT, and CS CCWs are procured from different power plants in Alabama, Georgia, Georgia, Mississippi, Wisconsin, South Carolina, Missouri, and South Carolina. This is intended to reflect the variability in the coal sources used nationwide.

CCW chemical and physical testing

The physical and chemical properties of the CCW are obtained through several tests. The Specific Gravity (SG) was measured with Le Chatelier Flask for Density per ASTM C188-17. The Rigden Voids test was conducted according to the European Standard EN1097-4. Particle Size Distribution (PSD) was determined according to ASTM D4464 using laser light scattering with alcohol solution instead of distilled water to avoid cementation and acquire more precise results. The laser light scattering results were used to calculate the specific Surface Area (SA), D_{10}, D_{50}, and D_{90} Parameters. The D_{10}, $D_{50,}$ and D_{90} can be defined as follows: D_{90} means the percentage of particles finer than this size is 90%. D_{10} means the percentage of particles finer than this size is 10%. D_{50} means the portion of particles with diameters smaller and larger than this value is 50%, also known as the median diameter. The chemical elemental analysis was obtained using X-Ray Fluorescence (XRF) following ASTM D6247- 18. In addition, the shape of the particle of fly ash was investigated using Scanning Electron Microscope (SEM).

Laboratory testing methods to evaluate binder blends

To evaluate an additive to the asphalt binder, it is necessary to quantify the change in the binder's fundamental behavior. To evaluate the claim that the CCW is acting as an additive, it is necessary to investigate the changes in the rheology of the asphalt binder to distinguish between the influence of inert particulate inclusion (filler) or an additive that contribute to the overall performance of the binder matrix. Laboratory methods reported for evaluating binder additives are numerous. For this paper, this section will focus only on the following methods:

1- Chemical analysis using Fourier Transform Infrared Spectroscopy (FTIR)
2- Full performance grading PG testing is conducted per AASHTO M320

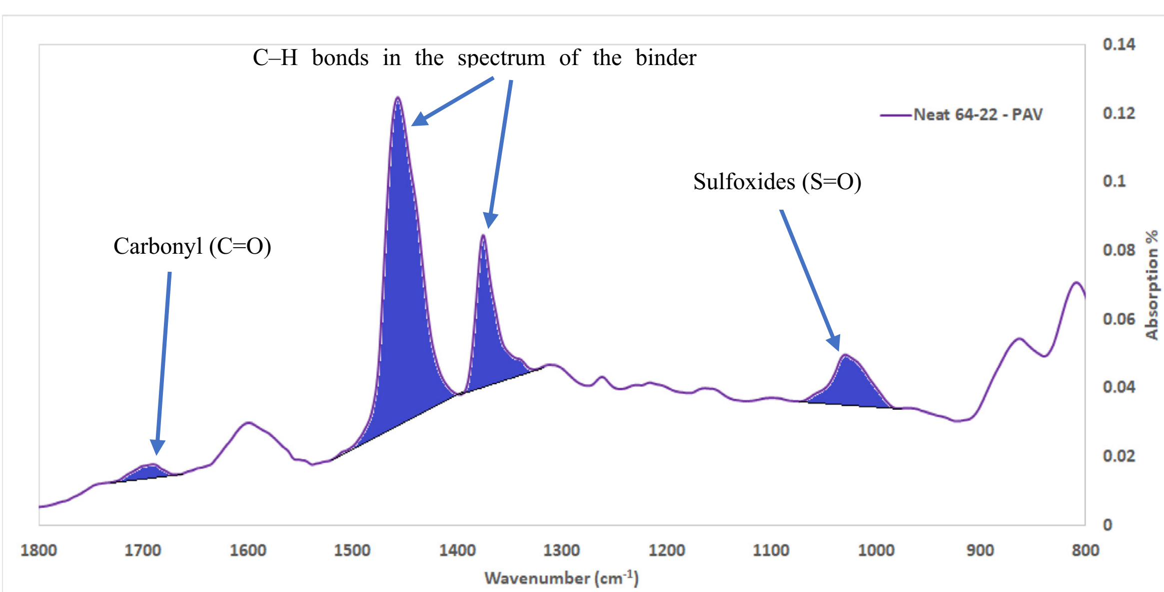

Fig. 1. Illustration of Determination of Peak Areas for the Unmodified Binder after PAV Aging.

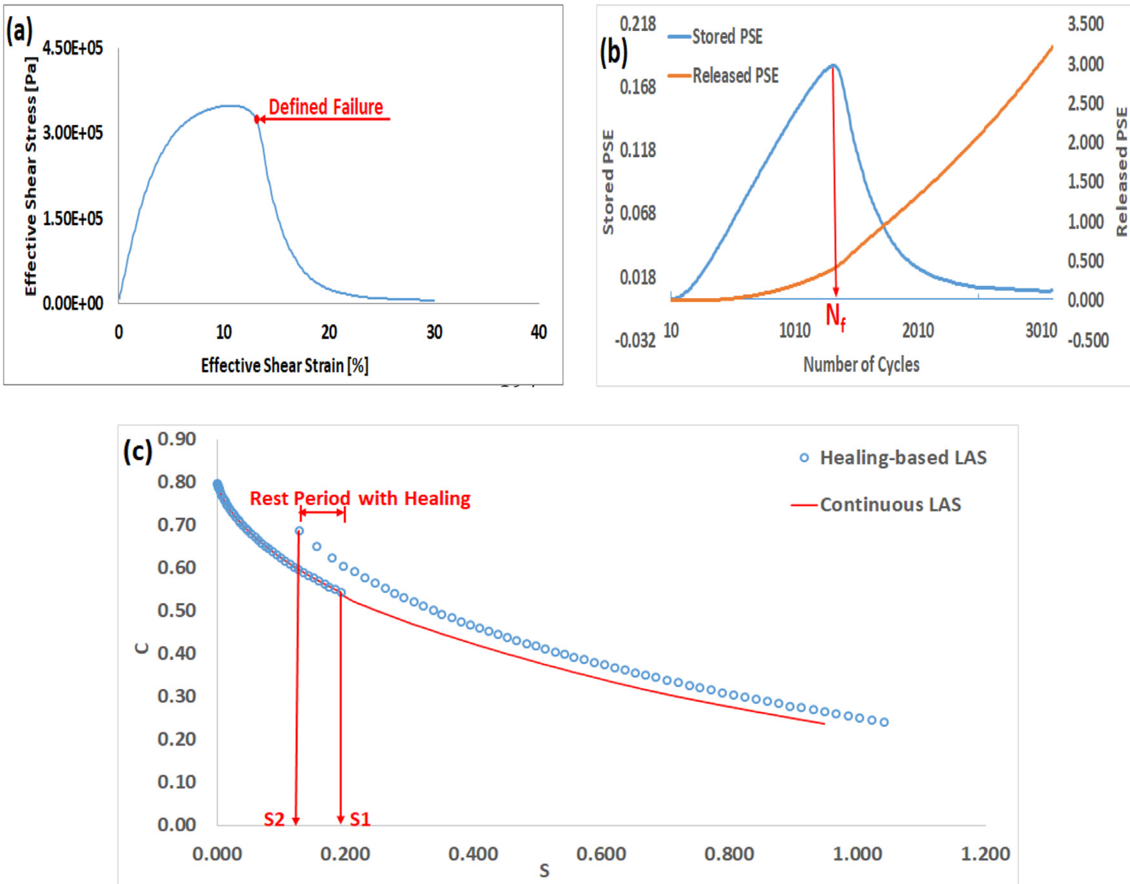

Fig. 2. Fatigue Failure in LAS Tests for the Unmodified Asphalt Binder: (a) Stress-Strain Curve, (b) PSE-Based Failure (After Wang et al., 2015), (c) Schematic Illustration for %Healing Calculation (After Xie et al., 2017).

3- Rheological analysis of time and temperature dependency using master curves using the dynamic shear rheometer (DSR)
4- Damage analysis and healing using the DSR.

Chemical analysis using FTIR

This method relies on passing a beam of infrared radiation through a sample, and a spectrometer analyzes the transmitted radiation. The spectrum of transmitted radiation, either in terms of transmittance or absorbance, shows absorbed radiations at specific wavelengths. This absorbed radiation at a particular wavelength corresponds to the absorbance due to vibration or rotation of a particular chemical bond when the frequency of vibration (or rotation) of the bond matches that of infrared radiation. Traditionally, the functional groups of carbonyl (C = O) and sulfoxides (S = O) are used to evaluate the asphalt binder and monitor its changes through different levels of oxidative aging. Many studies discussed using this method to evaluate chemical changes in the binder in the presence of additives *(*Lamontagne et al., 2001; FARCAS; et al., 2009; Wu et al., 2010; Yang et al., 2015; Singh, Saboo and Kumar, 2017; Nayak and Sahoo, 2017*)*. A detailed method for quantifying the carbonyl index (ICO) and the sulfoxide index (ISO) is reported by Grenfell et al. 2009. The authors proposed the following equations to calculate both indices:

$$ThecarbonylIndex(ICO) = \frac{Areaaround1700cm^{-1}}{Areaaround1460cm^{-1} + Areaaround1375cm^{-1}} \quad (1)$$

$$ThesulfoxideIndex(ISO) = \frac{Areaaround1030cm^{-1}}{Areaaround1460cm^{-1} + Areaaround1375cm^{-1}} \quad (2)$$

The numerator in previous equations corresponds to the peak area due to the stretching of ketonic bonds. The denominator in the Equation corresponds to the bending of C–H bonds in the spectrum of the binder sample. The relative area in a particular spectrum is considered instead of the height or magnitude of the peaks. The areas around the peaks of interest are calculated by constructing a baseline from valley to valley, as shown in Fig. 1.

Rheological time and temperature dependency

The master curves for the complex modulus (G*) and phase angle (δ) are constructed using DSR frequency sweep testing. For PG 64–22 binder/blends, testing is conducted at different temperature levels; 10 °C, 22 °C, 34 °C, 46 °C, 58 °C, 64 °C, and 70 °C covering a frequency range from 100 to 0.1 rad/s at each temperature. For PMA 76–22 binder/blends, the test was held at 10 °C, 22 °C, 34 °C, 46 °C, 58 °C, 70 °C, and 76 °C covering the same range of frequencies. The amplitude strain was set to 0.1% for both intermediate and high temperatures (10–34 °C, 46–76 °C) respectively to achieve linear viscoelastic range behaviors for the blends/binder tested. Two samples of each blend/binder are tested, achieving a Coefficient of Variation (COV) not exceeding 10%. The constructed master curves are then used to compare the different blends and calculate the crossover modulus G_c*.

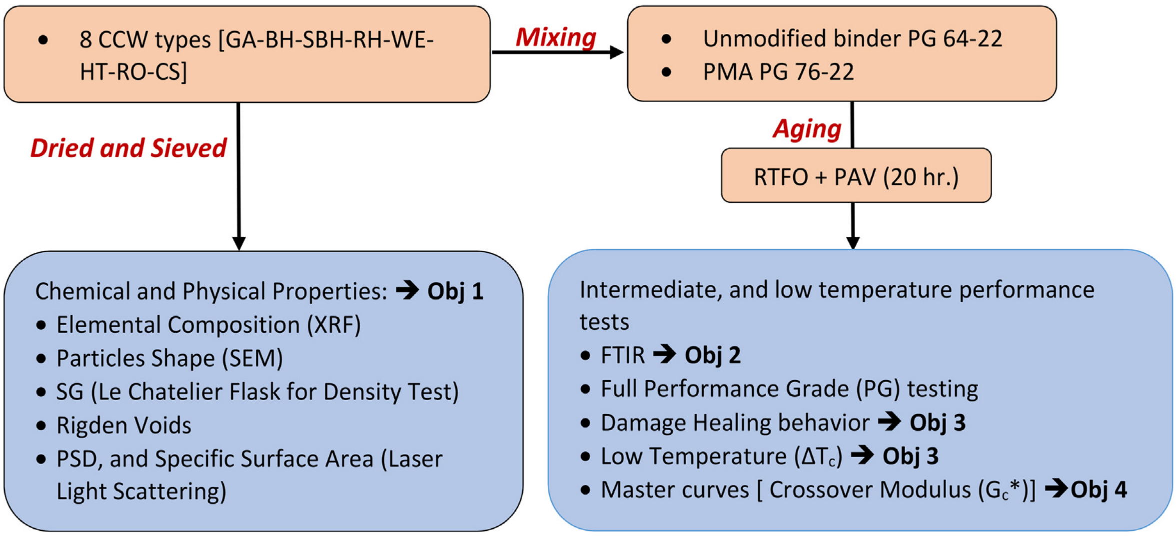

Fig. 3. Experimental Program.

Damage behavior

Studying the damage behavior of asphalt binders has received the attention of many researchers. Given the viscoelastic nature of the asphalt, it is necessary to study damage under different schemes. This paper will focus on damage and healing of the binder at a temperature range where the binder is behaving as a viscoelastic polymer (viscous and elastic components are equal).

Damage healing characterization

Xie et al. (2017) developed a new procedure based on a Linear (strain) Amplitude Sweep (LAS) test to quantify healing performance, as explained in Fig. 2. This protocol is a four steps procedure. First, a continuous LAS test is conducted at the intermediate temperature - determined as the intermediate temperature of the performance grade (PG). The first step is conducted to define the strain level where damage starts to occur. Second, a new binder sample is subjected to the LAS loading until it arrives at the specific strain amplitude corresponding to the previously determined damage level. Third, a rest period is applied while maintaining the temperature. Eventually, the LAS loading is resumed from the strain amplitude applied prior to the rest period. As demonstrated in Fig. 2-c, the percent healing (%Hs) can be quantified from the change in the accumulated damage growths through Equation (3), where S1 and S2 are damage intensities before and after applying the rest period, respectively.

Wang et al. (2015) developed a new approach to analyzing the data through simplified viscoelastic continuum damage (S-VECD). As described in Fig. 2-a and b, the new failure criterion analysis is based on Pseudo-Strain Energy (PSE). Wang et al. (2015) proved that trends in stored PSE effectively define the failure for the LAS tests of asphalt binders. Moreover, the new proposed failure definition is material-dependent, which makes it effective in capturing the change in binder behavior after the introduction of an additive.

$$\%H_s = \frac{S1 - S2}{S1} \tag{3}$$

Low-Temperature cracking susceptibility using bending beam rheometer BBR

This test follows creep loading of an asphalt beam at low temperature. This test is used to quantify the stiffness (S) of the binder under sustained loading as well as the rate of increase in stiffness (m). For practical reasons, the load is sustained for 60 s to record S(60 s) and m(60 s) as the parameters used to evaluate and compare binders' performances. The standard practice sets an acceptable level of S is < 300 MPa and for m-value is greater than 0.3. Anderson et al. (2011) introduced the ΔT_c parameter, the numerical difference between the critical low temperature corresponds to stiffness, S at 300 MPa, and critical temperature corresponds to the m-value of 0.300. In other words, ΔT_c is a numerical index value for gauging the binder's ability to compensate the increase in stiffness with relaxation. Some studies have suggested acceptable values for this parameter, a crack warning value of −2.5 °C was suggested by Anderson et al., and a cracking limit value of −5°C was suggested by Rowe when an identifiable risk of cracking for the binder occurs (Anderson et al., 2011; Rahbar-rastegar, 2017).

Experimental design

To achieve the objectives, an experimental design is illustrated in Fig. 3. Experimental tasks addressing the four objectives of the study are labeled accordingly. All asphalt blends are conditioned with rolling thin film oven (RTFO), then pressure aging vessel (PAV) for 20 h to induce oxidative aging.

Fabrication of blends

The process of blending starts with heating the PG-64–22 binder to 135 ± 5 °C, and the polymer-modified PG 76–22 binder to 155 ± 5 °C.

Table 1
Chemical requirements (ASTM C618-19).

	Class		
	N	F	C
Silicon dioxide (SiO_2) + aluminum oxide (Al_2O_3) + iron oxide (Fe_2O_3) [SAF], min, %	70.0	50.0	50.0
Calcium oxide (CaO), %	Report Only	18.0 max	greater than18.0
Sulfur trioxide (SO_3), max, %	4.0	5.0	5.0
Loss on ignition, max, %	10.0	6.0	6.0

Table 2
Chemical Elemental Composition and LOI of the Investigated Fly Ashes.

CCW	SiO_2, %	Al_2O_3, %	Fe_2O_3 %	SAF	CaO, %	SO_3, %	LOI, %	Class Interpretation
GA	52.02	22.42	15.54	89.97	3.00	0.82	0.93	**F**
BH	6.61	3.22	2.39	12.22	52.74	16.82	8.92	**OFA**
SBH	23.15	16.01	4.93	44.09	26.16	7.01	13.24	**OFA**
RH	41.77	17.40	3.69	62.86	22.41	6.48	1.77	**OFA**
WE	31.77	15.55	4.88	52.20	27.59	10.24	1.55	**OFA**
RO	57.57	25.63	10.49	93.68	0.90	0.08	3.87	**F**
HT	25.71	13.99	4.50	44.20	34.32	11.13	5.68	**OFA**
CS	39.04	21.84	3.04	63.92	16.94	13.24	3.52	**OFA**
Average	34.70	17.01	6.18	57.89	23.01	8.23	4.94	
OFA =	Off-spec Fly Ash							

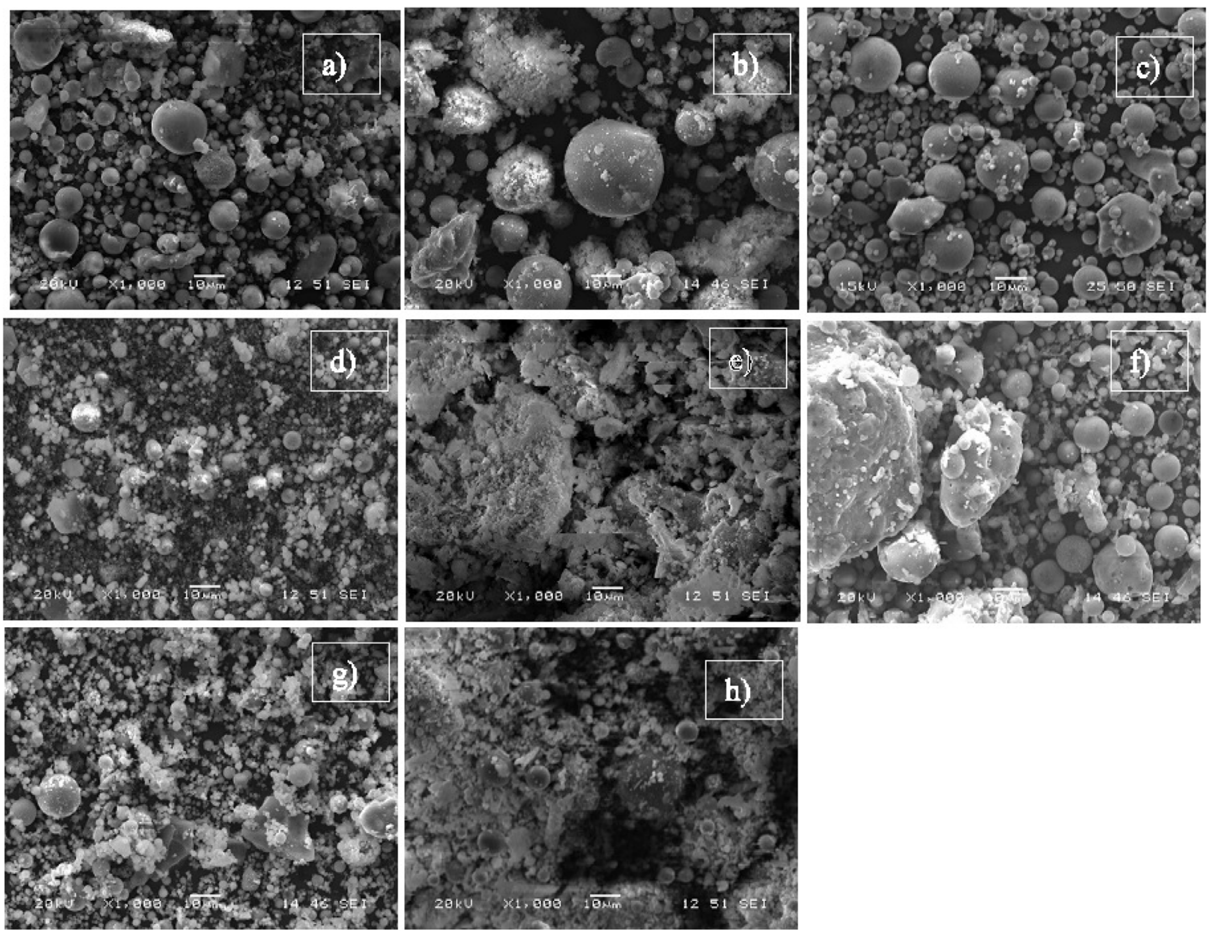

Fig. 4. SEM of Samples at 1000x Magnification: (a) BH (b) CS (c) GA (d) HT (e) RH (f) RO (g) SBH (h) WE.

Table 3
Physical Properties of Fly Ash.

Coding Name	Fly ash class	Specific gravity (g/cm^3)	Rigden Voids %	D_{10} (μm)	D_{50} (μm)	D_{90} (μm)	Specific Surfacearea (cm^2/g)	D_{90}-D_{10} D_{50}
GA	F	2.47	28.89%	1.00	11.70	64.40	28,179	5.42
BH	Off-spec	2.40	56.85%	1.30	6.75	220.95	18,339	32.54
SBH	Off-spec	2.39	42.37%	0.90	12.00	106.90	29,405	8.83
RH	Off-spec	2.58	56.76%	2.50	26.10	95.65	13,568	3.57
WE	Off-spec	2.64	34.25%	1.00	23.30	113.00	24,293	4.81
RO	F	2.30	38.15%	2.53	28.65	103.85	15,042	3.54
HT	Off-spec	2.59	42.20%	1.00	6.95	133.80	26,959	19.11
CS	Off-spec	2.25	48.20%	3.40	31.20	63.50	13,677	1.93
Average	———	2.45	43.46%	1.71	18.32	112.75	21,183	9.97

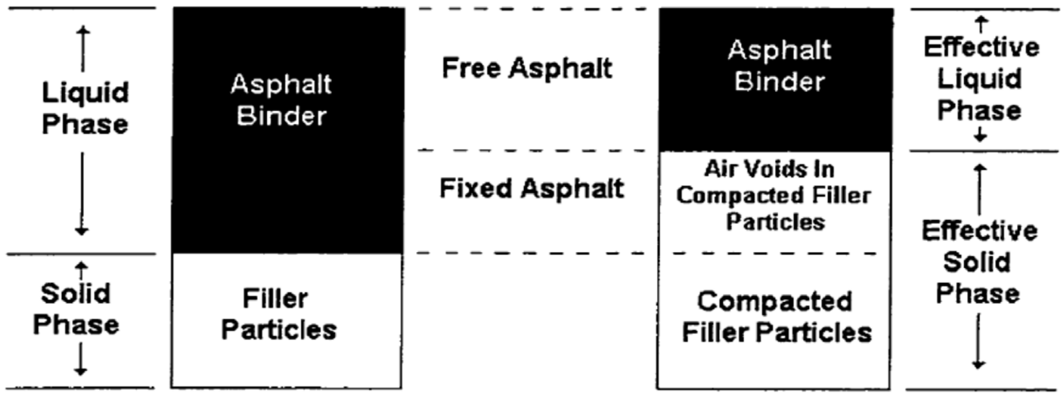

Fig. 5. A Schematic Showing the Concept of Fixed Asphalt and Free Asphalt [Smith, 2001].

CCWs are heated to the same temperatures as binders before blending. The CCW sample is loaded incrementally to the binder and dispersed using a high shear mixer. The blending process is completed in 30 min. This process yielded 16 blends; 8 CCW blended with two binders. It is important to mention that the un-blended control samples are exposed to the same protocol to avoid fabrication/conditioning bias.

Testing results and discussion

In this section, the results are presented in three parts. The first part discusses the chemical and physical characterization of CCW. Further, the second section discusses the blend's performance. Finally, the second part is coupled with regression analysis to identify the statistically significant parameters influencing the reported results.

Chemical and physical characterization of fly ash

CCW chemical composition

As shown in Table 1, the ASTM C618-19 determines the limits for classifying the different types of fly ash.

The results from the XRF test are reported in Table 2. Comparing the composition of the CCW samples tested to Table 1 for classification results in identifying GA and RO as Class F fly ash. The remaining is classified as OFA.

Particle shape and size distribution of fly ash

Scanning electron microscope (SEM) images are presented in Fig. 4. Standard classes of fly ash (Class C and Class F) are typically characterized by their spherical shapes, as shown in Fig. 4c and 4f. All the OFA contain a mix of spherical and irregular shapes. The differences in the coal-burning processes can be the main reason for the variation in the fly ash shape (Sinsiri et al., 2010). In addition, per the supplying utilities, some of the OFA are residual material created from the combination of fly ash and the reagent lime from the scrubber unit used to absorb acidic exhaust gases. Samples belonging to this class are demonstrated in Fig. 4d and 4 g. These materials are referred to as Spray Dryer Absorber (SDA).

Table 3 demonstrates the D_{10}, $D_{50,}$ and D_{90} as estimated from the particle size distribution data. This information is obtained based on conducting laser diffraction (ASTM D4464-10) on the samples. A group of CCWs (SBH, GA, WE, and HT) is characterized by the presence of very fine particles. This is demonstrated by the size of D_{10} falling within the 0.94–1.02 μm size range.

The specific surface area (SA) obtained from the same test is considered surrogate to the particulates' binder adsorbing capacity. Generally, the SA of powder particles varies inversely with the particle size; the larger the surface area, the finer the particle distribution, and the greater the binder adsorbing capacity. Table 3 shows the specific surface area. It is noticed that the SA of BH, RH, RO, and CS fly ash are below the average, indicating that they are on the coarser side. Finer CCW (GA, SBH, and HT) exhibit higher SA values as expected.

Table 4
Continuous Performance Grade for Unmodified and PMA Blends.

	Unmodified binder PG 64–22			PM binder PG 76–22		
Continuous PG	PGH	PGL	PGI	PGH	PGL	PGI
Control Binder	67.40	S −26.70		79.40	S −25.63	
		m −25.66	22.95		m −24.90	23.70
GA	68.80	S −24.89		80.95	S −24.96	
		m −25.44	23.70		m −25.45	22.45
BH	70.00	S −24.40		83.00	S −22.90	
		m −24.36	24.00		m −23.08	25.70
SBH	69.00	S −23.56		81.85	S −24.28	
		m −25.72	23.65		m −25.10	24.25
RH	68.90	S −23.89		81.75	S −24.20	
		m −26.34	23.15		m −22.85	25.40
WE	68.20	S −24.51		81.10	S −24.53	
		m −26.49	23.00		m −24.88	24.85
RO	69.00	S −24.61		81.80	S −25.43	
		m −25.43	23.20		m −25.01	24.80
HT	69.30	S −24.26	24.10	81.70	S −24.05	25.25
		m −24.95			m −24.96	
CS	69.40	S −23.86	25.05	82.65	S −24.45	23.80
		m −24.50			m −24.57	

Fractional voids (Rigden Voids)

The capacity of the particulates to hold asphalt binder can be estimated using the voids entrapped in a compacted sample of filler. The void content is estimated by compacting dry fillers in a mold using a specified compaction effort. The concept is similar to the Fine Aggregate Angularity test utilized in the Superpave system to measure the angularity of fine aggregates (AASHTO 304), but includes a standard compaction device to pack the filler. In 1947, Rigden introduced the measurement of fractional voids Rigden (1947). Hence, most researchers refer to the fractional voids test as the “Rigden Voids” test (Anderson and Goetz, 1973, Anderson et al., 1982).

Rigden considered the asphalt required to fill the voids in the dry compacted sample as fixed asphalt, while excess asphalt is considered free asphalt. Rigden postulated that the percent free asphalt is the main factor defining the consistency of filled systems and reported that changes in viscosity are independent of asphalt characteristics or any particulate characteristics other than the fractional voids. Based on these findings, it was concluded that the chemical differences between various particulates are of less significance. Fig. 5 illustrates the concept proposed by Rigden.

The results of the Rigden Voids test reported in Table 3 show a wide range of values. The maximum value is associated with BH at a value of 56.85%, which also possesses the coarsest particles. The minimum value is associated with GA at 28.89%. It is also among the finest of the CCWs studied. Based on Rigden’s stipulation, these two CCWs should be the most and least influential, respectively, when blended with the binders.

The following sections discuss whether the CCW included in this study follows Rigden's postulation. The CCW will act as fillers if their effect on the binder is directly correlated to their physical properties and inclusion load. The literature studies discussed in the introduction of this paper suggest that some classes of CCWs deviate from acting as fillers. This study will add to this knowledge body and demonstrate the rheological changes in the blended system due to the presence of the CCWs. To achieve this goal, the selected CCW selected for testing are showing a wide range of compositional and physical properties to such that the changes in the properties of the system can be studied and correlated to the CCW characteristics.

Asphalt blends performance

Superpave performance grading results

In Table 4, the continuous Performance Grade (PG) is presented. The high PG (PGH) is determined using the Superpave parameter of G*/sinδ. The low PG (PGL) is determined using the BBR Superpave stiffness (S) and relaxation (m) parameters. The PGH represents the maximum summer temperature the blend can be employed. Similarly, the PGL is related to the lowest winter temperature before failure occurs in the binder. Finally, intermediate PG (PGI) is measured using the DSR where it corresponds to the temperature at which G*.sinδ is equal to 5000 kPa. The lower PGI is commonly interpreted as higher fatigue resistance since it is indicative of the ability of the system to maintain flexibility under repeated loading.

Following the influence of the CCW on each binder, for the PG64-22 binder, the true high grade deviated from the control binder by at most + 2.6 °C with BH blend. This deviation changed the high standard grade to PG70. The rest of the blends show a minimal increase in the high grade not exceeding + 2 °C. For the PGI, all the blends increased in value. The blend with CS shows the most increase of 2.10 °C. The remainder of the blends shows a less stiffening effect, with a maximum increase of 1.15 °C for the blend with HT. The least

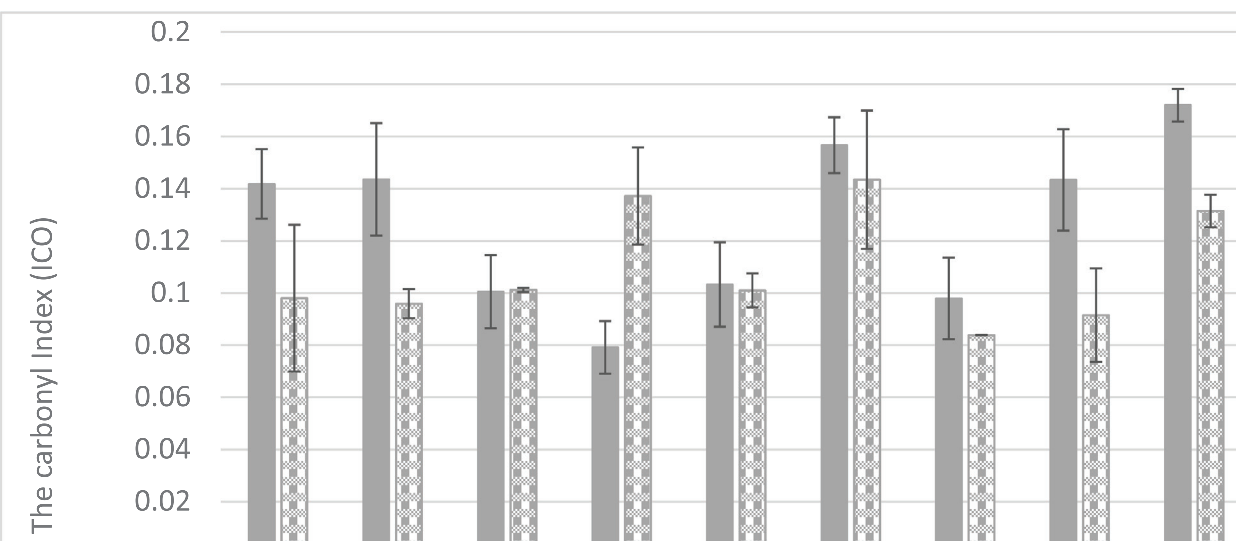

	GA	BH	SBH	RH	WE	RO	HT	CS	Control Binder
Neat 64-22	0.142	0.144	0.100	0.079	0.103	0.157	0.098	0.143	0.172
PMA76-22	0.098	0.096	0.101	0.137	0.101	0.143	0.084	0.092	0.131

Fig. 6. The Carbonyl Index (ICO) of the Investigated Blends/Binders.

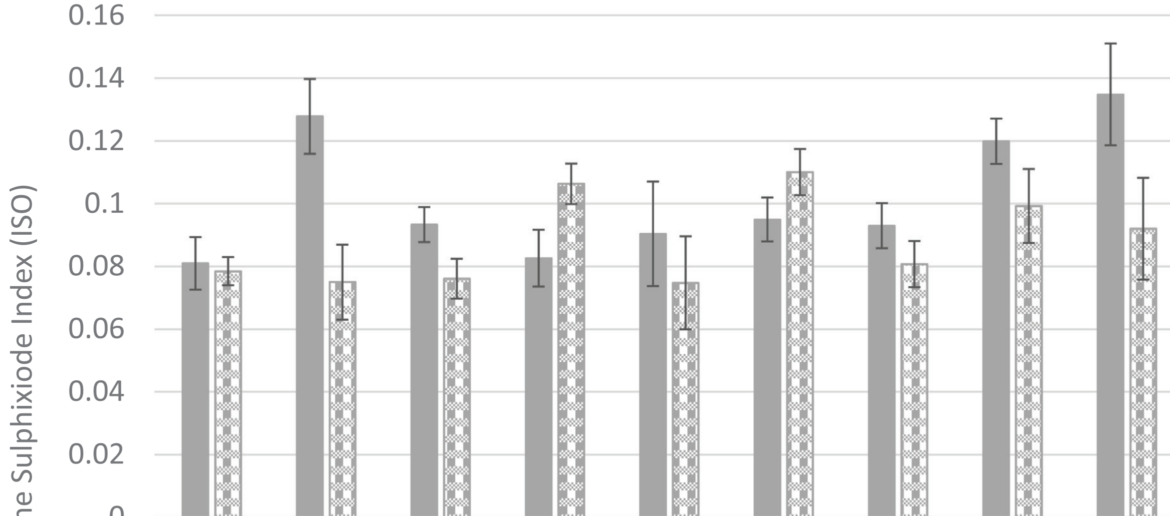

	GA	BH	SBH	RH	WE	RO	HT	CS	Control Binder
Neat 64-22	0.081	0.128	0.093	0.083	0.090	0.095	0.093	0.120	0.135
PMA76-22	0.078	0.075	0.076	0.106	0.075	0.110	0.081	0.099	0.092

Fig. 7. The Sulfoxide Index (ISO) of the Investigated Blends/Binders.

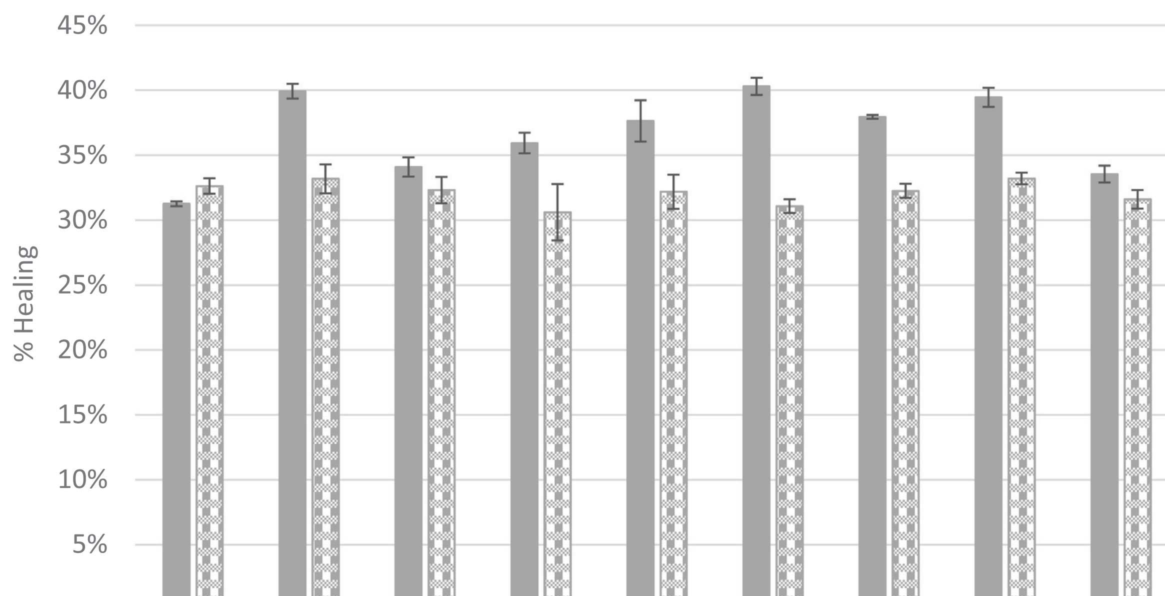

	GA	BH	SBH	RH	WE	RO	HT	CS	Control Binder
Neat 64-22	31.26%	39.93%	34.08%	35.93%	37.64%	40.31%	37.95%	39.46%	33.54%
PMA76-22	32.62%	33.18%	32.31%	30.61%	32.18%	31.08%	32.25%	33.20%	31.60%

Fig. 8. Healing Performance of the Investigated Blends/Binders.

increase is the blend with WE, which shows a minimal increase of 0.05 °C. For PGL, the critical temperature associated with the stiffness increased for all blends. The maximum increase is associated with SBH, where the critical temperature increased from −26.70 °C for the control blend to –23.56 °C for the blend with SBH. Interestingly, the associated for the critical temperature relaxation index (m-value) showed a decrease from −25.66 °C to −25.72 °C. This is a minor difference; however, it indicates that while the blend increased in low-temperature stiffness, it did not lose its ability to relax thermal stresses. Therefore, given that both the control and the SBH blend are graded as PG64-22, the SBH blend is expected to show superior resistance to cracking given its higher m-value.

The same trend is observed for the PMA PG76-22 for the true high grade. The maximum increase in the PGH is associated with the BH blend at + 3.6 °C. This increase changes the standard grade to PG82. The other blend that changed grade is the blend with CS, where the PGH changed by 3.25 °C. The remainder of the blends maintained the same grade. For PHI, the maximum increase is observed with the BH, RH, and HT blends. It is interesting that most of the remaining blends are hovering around the value of the control within a range of 1.00 °C. In fact, the blend with GA shows a PGI of −1.25 °C less than the control. For the PGL, all the blends show a minimal increase in the critical temperature associated with the stiffness. On the other hand, a group of blends (GA, SBH, WE, and HT) shows improvement in the thermal relaxation index (m-value).

It is important to note that the maximum increase in the PGH for both binders is associated with the BH blend. The BH CCW possesses the highest value of the Rigden voids at 56.9%. Therefore, this is aligned with the postulation of Rigden and other researchers. However, the stiffness measures at the intermediate and low temperatures show different trends. A CCW with a similar Rigden voids value is RH at 56.8%. The blend with this CCW is associated with a much lower increase in stiffness as measured by the PGH and PGI, comparable to values similar to other CCWs with lower Rigden voids values. For example, the PGH for RH with the PG64 binder is 68.9 °C, and the PGH for GA is 68.8 °C. Noting that the GA has the lowest Rigden voids value at 28.9% contradicts Rigden's postulation. Furthermore, the blend with the RH improved is associated with an improved low-temperature relaxation at low temperature for the same binder, while GA is associated with a small reduction in relaxation. This could mean that BH acts as a filler while the RH interacts with the binder and enhances its performance.

Analysis of infrared spectroscopy (FTIR)

Carbonyl and Sulfoxide Indices are shown in Figures-6 and 7, respectively. The data shown are the average of four specimens. The spectral peaks of interest for the sulfoxide peak were 1030 cm^{-1} and the carbonyl peak at 1700 cm^{-1}. To analyze the carbonyl and sulfoxide groups with the presence of fly ash, these spectra are normalized using a reference of bending of C–H bonds in the spectrum of the binder sample. The higher the carbonyl and sulfoxide indices, the higher the level of oxidative aging. As shown in Fig. 6, the presence of fly ash with the unmodified binder is associated with reduced levels of ICO by a range of −54%, with RH fly ash, to −17% with CS fly ash.

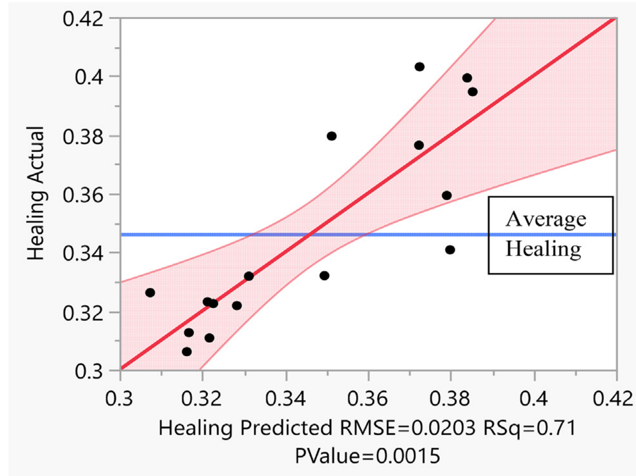

Fig. 9. Comparison of measured damage healing performance against predicted values.

For the PMA blends, the presence of the CCWs, except with RO and RH, is associated with reduced ICO by a range varying from −36% with HT fly ash to –23% with SBH. The two CCWs not associated with a reduction in the ICO for the PMA are associated with a small increase. RO is associated with a + 9.16% increase in the ICO, while RH is associated with an increase of + 4.58% only.

Analyzing sulfoxide index (ISO) data demonstrated in Fig. 7 shows the same trend. For the unmodified binder, all CCWs are associated with a reduction in the ISO by a range of −40%, with GA, to −5% with BH. For the PMA blends, the presence of fly ash, except with RO, RH, and CS, also reduced the oxidative aging index by a range that varies from −19% with WE fly ash to −12% with HT fly ash. The increase in the ISO associated with RO, RH, and CS is 19.57%, 15.22%, and 7.61%, respectively. As can be noted, both RO and RH negatively affect the aging indices of the polymer-modified binder. This may suggest that the inclusion of these particulates in a system already loaded with polymer causes some negative interaction. These results are not conclusive at this stage, but the only common property for these CCW is that they possess the smallest specific surface area and the tightest size range as measured by $\frac{D_{90}-D_{10}}{D_{50}}$. Further testing will focus on these CCWs to evaluate if particle size distribution plays a role in the blend performance.

Damage healing evaluation

Fig. 8 demonstrates the results of the healing test for both binders. For the unmodified binder blends, the addition of all the CCWs is associated with an increase in the healing capability, except for GA. BH, RO, and CS are associated with the highest level of healing of about 20% more than the control binder. All the other blends are associated with more than a 10% increase in healing.

For the PMA blends, the damage healing results show minimal change compared to the control binder. That is expected as some

Table 5
Results of the Healing performance regression multivariate analysis.

Term	Estimate	Std Error	t Ratio	Prob>|t|
Intercept	−0.6051	0.2327	−2.6000	0.0232
SO_3, %	0.0029	0.0009	3.0738	0.0096
Specific Gravity (g/cm^3)	−0.0968	0.0394	−2.456	0.0303
Phase angle (δ) at intermediate temperature ()	0.0239634	0.0048	4.9401	0.0003

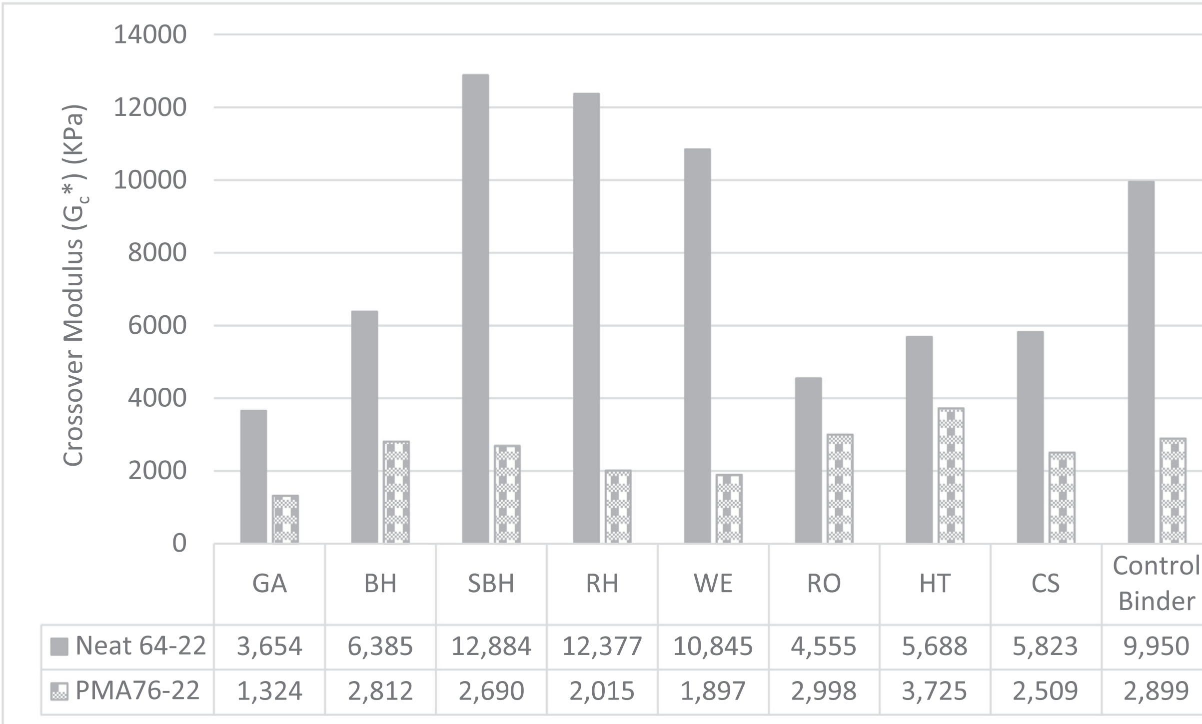

Fig. 10. Crossover modulus (G_c*) of the investigated blends/binders.

Table 6
Results of the crossover modulus regression multivariate analysis.

Term	Estimate	Std Error	t Ratio	Prob > |t|
Intercept	−133283.1473	20129.9929	−6.6211	< 0.0001
SiO_2, %	−83.0078	29.94235	−2.7723	0.0158
Phase angle (δ) at intermediate temperature ()	2907.4419	417.6719	6.9611	< 0.0001

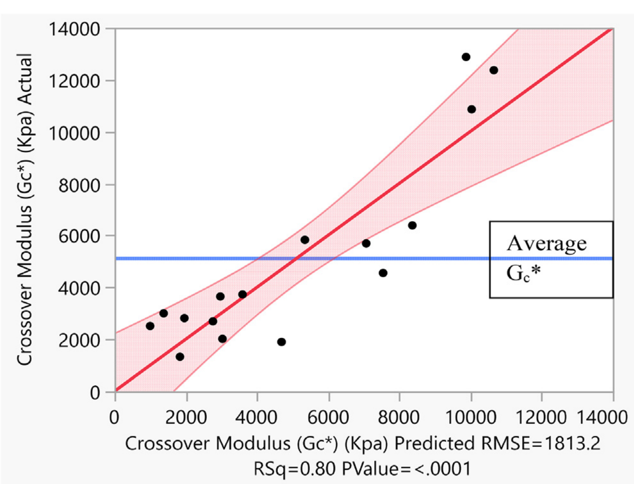

Fig. 11. Comparison of measured crossover modulus against predicted values.

polymer-modified binders tend to show a higher degree of stiffening due to aging. SBS modified binder is found to be prone to molecular breakdown due to oxidation, which leads to significant loss of the elastic recovery response (Xu et al., 2017, Yu et al., 2019). Therefore, the healing capacity may be affected by the polymer.

The difference in response between the two binders indicates that the damage healing mechanism is dominated by both the binder and the added CCW. It also illustrates that the interaction of the CCW and the polymer may be a critical factor. To quantify the interaction, regression analysis is used to identify statistically influential parameters.

Fly ash Physio-chemical influence on asphalt binder's healing performance

Given the results presented in Fig. 8, it is expected that the regression analysis will reveal both binder and CCW properties as the significant factors influencing healing. The details of the regression model are shown in Table 5. As expected, the formulation of the model relies on the phase angle of the binder/blend after aging as the most significant independent variable, as demonstrated by the p-value. The model also reveals that SO_3%, specific gravity of the CCW are significant parameters influencing the damage healing.

As seen in Fig. 9, the regression model values are in solid agreement with the measured values. Examining the regression parameters, the coefficients of the independent variables follow expected trends and follow fundamental materials principles. It is essential to comment on having the phase angle of the blend as part of the model. In typical particulate viscoelastic composites, the particulates' presence is associated with an increase in stiffness and reduction in phase angle. This is due to the differential flow of the matrix and the particulates in the blends. However, the phase angle is a good measure of synergy when the particulates contribute to the flow. Therefore, the inclusion of such

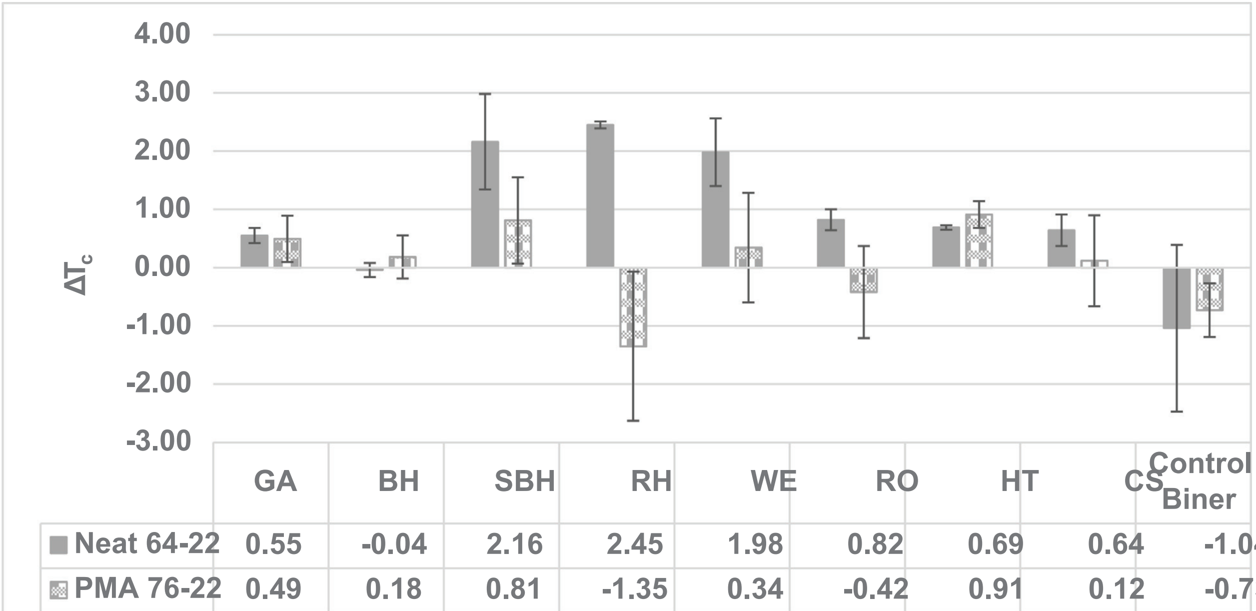

Fig. 12. Low temperature cracking potential of the investigated Blends/Binders.

parameters in the model serves as a strong indication of the ability of the particulate additive to contribute to the overall blend performance. As for sulfur, it has been reported in many studies that it has softening effect on asphalt and increases durability (Cha et al., 2009; Parvez et al., 2014; Abdullah and Wahhab, 2015; Polacco et al., 2015; Le et al., 2020; Singh et al., 2020). Accordingly, showing up in the regression model as a significant parameter conforms with the reports from other researchers. The statistical results confirm the stipulation that the CCW influences the blend as an additive, not as a filler.

Crossover modulus (G_c)*

The crossover modulus is a valid rheological parameter to quantify the change in the material. Crossover modulus is defined as the complex shear modulus when the phase angle equals 45°, where the storage modulus equals the loss modulus. It has been used as means to evaluate the influence of additives on binders' aging behavior. The crossover modulus is inversely related to aging (Farrar et al., 2013). In this study, the crossover modulus (G_c*) was determined from the master curves of complex shear modulus and phase angle through frequency sweep tests. The reference temperature was chosen as 15 °C in this study. Two samples of each blend/binder were tested in the DSR frequency sweep test achieving a Coefficient of Variation (CoV) not exceeding 10%.

Fig. 10 shows the crossover modulus of the investigated blends/binders. For blends based on the unmodified binder, the addition of SBH, RH, WE are associated with an increase in G_c* of 29%, 24%, and 9%, respectively. On the other hand, the remaining CCWs are associated with a reduction in the G_c*. For the PMA's blends, only HT and RO show improvement. The G_c* increased by 28% and 3%, respectively. Examining both healing and G_c*, HT is associated with improved performance, and it is among the finest ash used as determined by its specific surface area. Regression analysis is used to highlight the statistically significant parameters influencing the observed results.

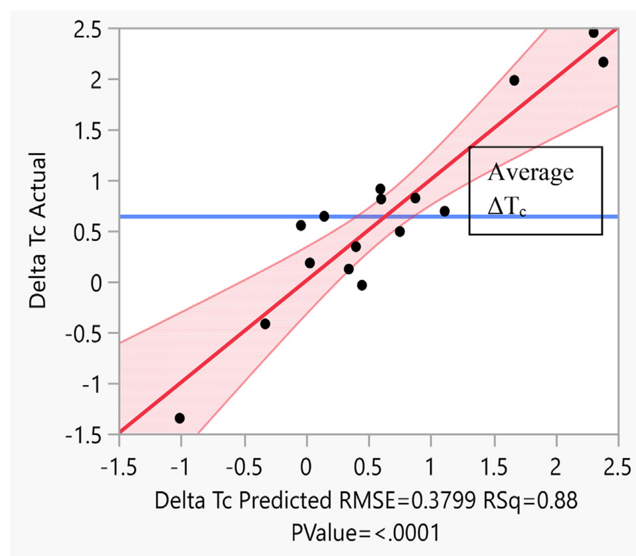

Fig. 13. Comparison of measured ΔT_c against predicted values.

Table 7
Results of the ΔT_c regression multivariate analysis.

Term	Estimate	Std Error	t Ratio	Prob > |t|
Intercept	–22.8164	4.3151	−5.2875	0.0003
Specific Gravity (g/cm^3)	−3.3321	0.9805	−3.3981	0.0059
D_{10} (μm)	−0.3497	0.1327	−2.6349	0.0232
The carbonyl Index (ICO)	−24.5841	4.4057	−5.5801	0.0002
Phase angle (δ) at intermediate temperature ()	0.7207	0.0925	7.7913	<0.0001

Fly ash Physio-chemical influence on asphalt binder's aging indicator (G_c)*

The regression analysis reveals a high correlation between SiO_2% and the blend measured Phase angle after one cycle of PAV at intermediate temperature. The regression results are shown in the following Table 6.

Table 6 shows the significance of the two independent variables, silicon (Si) and the phase angle (δ). While the model shows a strong correlation power, as demonstrated by the high R^2 value of 80%, it also conforms with the healing model in showing the phase angle as the most critical parameter for capturing the physio-chemical influence of the CCW. On the other hand, the significant contribution of the Si conforms with reports from the literature. It has been reported by Zhang et al. (2019) and Guo and Tan (2021) to be a significant factor in the interaction between the particulates and asphalt binder.

Fig. 11 compares the asphalt blends' crossover modulus's predicted value for both unmodified and PMA binders against the measured values shown in the following plot. This comparison tests the strength of the fit. It is important to note that the presentation of such a figure illustrates the distribution of the data along with the range of G_c*. While the correlation coefficient is an important parameter in measuring the statistical fit, examining the distribution of the data reveals additional information. The data points are well distributed around the line of equality and around the average value. More importantly, the correlation does not seem to be influenced by a subset of the data points. This confirms that the crossover modulus significantly depends on the parameters in the model. This continues to confirm that some of the CCWs are not acting as fillers, but their interaction with the binder can improve performance as additives.

Low-Temperature performance evaluation

The ΔT_c is used for evaluating cracking potential at low temperatures for aged binders. The lower the value ΔT_c, the lesser the ability of the binder to relax the thermal stresses. In addition, the higher the level of aging, the lower the value of the ΔT_c. Therefore, this parameter has been used as a measure to evaluate the ability of additives to retain the binder's flexibility under different levels of aging (Lesueur et al., 2021). Fig. 12 demonstrates the results of this test for both binders. It is worth mentioning that although the CoV is high for the measured ΔT_c, both the critical low temperature corresponds to stiffness, S at 300 MPa, and critical temperature corresponds to the m-value of 0.300 did not exceed CoV 6.0%, which indicates high testing repeatability.

The results of the ΔT_c parameter continue the trend of mixed results based on the binder type. The most significant increase in the ΔT_c for the unmodified binder is found for RH, followed by the WE. In general, all blends maintained a ΔT_c value close to zero or above, indicating that they maintained their low-temperature thermal stress relaxation even after long-term aging. More importantly, they all show improved results compared to the control binder. Evaluating the PMA blends, some of the blends show improved ΔT_c after aging by more than 200%. In general, most blends show either preserve the binder ΔT_c or improve it. The only blend that is not associated with improved performance is the one with RH.

The results confirm the trend of previous observations that the interaction between some of the CCWs products and the asphalt binder reduces the detrimental effects of aging, which is believed to preserve the binder's ability to resist potential thermal cracking. Combining the observations from healing and resistance to cracking after aging reveals a very promising trend.

Fly ash Physio-chemical influence on asphalt binder's Low-Temperature performance (ΔT_c)

For ΔT_c, the regression analysis reveals that it is highly correlated to D_{10}, specific gravity, the carbonyl Index (ICO), and the measured blend phase angle after one cycle of PAV at intermediate temperature. The regression results are shown in the following Table 7.

Fig. 13 compares the predicted value of the ΔT_c for both unmodified and PMA binders against the measured values in the following plot. The Figure shows a high level of coefficient of correlation at 88%. However, R^2 should not be the only gauge for significance for a regression model. Examining the significant parameters used in the model, they include ash physical properties (Specific Gravity and D_{10}), a measure of blend aging sensitivity (ICO), and a measure of the viscoelastic interaction of the ash and the binder represented by the phase angle (δ). More importantly, the contribution of each of these parameters follows the expected scientific fundamentals of materials science.

Recommended future work

From sustainability point of view, most of the CCW used in this testing program are off-spec fly ash; they do not follow standardized formulation. Therefore, these CCW typically are deposited in landfills, underutilized. The results of this study provide strong evidence for the prospect of upcycling some off-spec CCW to be utilized as a high-value additive in the asphalt industry. The findings of this study must be complemented with mixture-level testing with CCW introduced as an additive rather than a filler. This means that the particulates will be incorporated as a part of the binder phase and not the aggregate phase. Therefore, no change in the job mix formula is anticipated. Therefore, the synergy of different CCW types should be considered to achieve higher performance for future work.

The storage stability of the blended binder is recommended to be studied as part of the CCW's feasibility to be utilized as an asphalt binder additive. Especially when aiming for mass production. Moreover, the interaction of fly ash with Reclaimed Asphalt Pavement (RAP) and Reclaimed Asphalt Shingles (RAS) is currently underway to validate that fly ash can reduce the aging rate.

A complete life cycle assessment (LCA) is necessary to quantify the reduction in energy and waste due to utilizing the appropriate type of CCW. This highlights the importance of this study and other studies in this area, as they formalize the appropriate type and properties of ash suitable for asphalt mixes.

Conclusion

The results and analysis presented in this paper show that significant improvements in asphalt performance can be attained in the presence of some types of CCW. The testing program is designed to study the hypothesis that some CCWs can act as an additive to the asphalt binder. The results show that improvement in binder performance can be attained depending on the CCW used.

The following points summarize the concluding statements of this study:

1- The presence of the particulates increases the stiffness of all the blends. This follows findings in the literature and the fundamental behavior of viscoelastic particulate composites.
2- The oxidative aging of most of the blends indicates retardation in aging. This is a critical finding. In fact, the results suggest that the mechanistic improvement in the blends is due to the retardation in aging. This means that the delay in aging allows the binder to maintain its flexibility, and durability is one of the influencing mechanisms of the CCW/Binder interaction. For example, all the blends exhibiting a consistent reduction in the aging indices are associated with the most improvement of in the low-temperature relaxation measured by the ΔT_c.
3- The interaction between the binder and the CCW is also measurable by the phase angle of the blend. It is the most statistically

significant parameter in all the regression models presented. This parameter is fundamentally a true reflection of the rheological change in the blends.

4- The combination of aging and the measured phase angle can be proposed as criteria for screening the CCW to distinguish between potential additives and fillers. The screening can be found valuable if the CCW is intended for implementation and commercialization. This is especially critical given the large quantity already deposited in landfills worldwide.

5- According to the results shown in this paper, three of the CCW used are associated with a significant change in the overall performance. These are HT, WE, and SBH. All three of these CCWs are considered off-spec and would end up in landfills. The other CCWs appear to act as fillers with some indications of conditional interaction depending on the binder used.

Declaration of Competing Interest

The authors declare the following financial interests/personal relationships which may be considered as potential competing interests: This study was performed under the currently ongoing The Electric Power Research Institute, Inc. (EPRI) Project: Utilization of Off-Spec Fly Ash as Aging Retarder for Asphalt Based Products.

Acknowledgment

The authors acknowledge the Electric Power Research Institute (EPRI) funding for this research work. The authors would like specially thank Ken Ladwig and Benjamin Gallegher for their support and guidance.

References

ACAA, 2020. Fly ash use in concrete increases slightly as overall coal ash recycling rate declines. (ACAA), Am. Coal Ash Assoc. d, 1–5.

Abdullah, Gamil M.S., Al-Abdul Wahhab, Hamad I., 2015. Evaluation of foamed sulfur asphalt stabilized soils for road applications. Constr. Build. Mater. 88, 149–158.

Anderson, D.A., Goetz, W.H., 1973. Mechanical behavior and reinforcement of mineral filler-asphalt mixtures. Joint Highway Res. Project, 37–66.

Anderson, D.A., Tarris, J.P., Brock, J.D., 1982. DUST collector Fines and their influence on mixture design. Assoc. Asphalt Pav. Technol. Proc. 51, 363–397.

Anderson, R.M., King, G.N., Hanson, D.I., and Blankenship, P.B., 2011. Evaluation of the Relationship between Asphalt Binder Properties and Non-Load Related Cracking. *Asphalt Paving Technology*, 80, Asphalt Paving Technology 2011.

Bautista, E.G., 2015. Experimental Evaluation of the Effect of Coal Combustion Products on Constructability , Damage, and Aging Resistance of Asphalt Mastics. *Ph.D. Dissertation.* University of Wisconsin Milwaukee.

Bautista, Emil G., Flickinger, Justin, Saha, Rajan, Flores-Vivian, Ismael, Faheem, Ahmed F., Sobolev, Konstantin, 2015. Effect of Coal Combustion Products on high temperature performance of asphalt mastics. Constr. Build. Mater. 94, 572–578.

Cha, A.E., Herrera-alonso, M., Herrera-na, R., 2009. Comparative study of the effect of sulfur on the morphology and rheological properties of SB- and SBS-modified asphalt. J. Appl. Polym. Sci. 10 (1002), 3409–3422.

Clopotel, Cristian, Velasquez, Raul, Bahia, Hussain, 2012. Measuring physico-chemical interaction in mastics using glass transition. Road Mater. Pav. Design 13 (sup1), 304–320.

Cloutier, C., Bautista, E.G., Faheem, A.F., Konstantin, S., 2017a. Effect of Spray Dryer Absorbers as Mix Enhancer on HMA Performance. In: International Congress and Exhibition" Sustainable Civil Infrastructures: Innovative Infrastructure Geotechnology, pp. 80–95.

Cloutier, C., Bautista, E.G., Faheem, A.F., Sobolev, K., 2017b. Effect of Spray Dryer Absorbers as Mix Enhancer on HMA Performance. In: International Congress and Exhibition" Sustainable Civil Infrastructures: Innovative Infrastructure Geotechnology, pp. 80–95.

Faheem, A., Bahia, H., Hintz, C., Al-Qadi, I.L., Reinke, I., Dukatz, E., 2010. Test Methods and Specification Criteria for Mineral Filler Used in HMA. (Final Report 9–45). Prepared for national cooperative highway research program. Transport. Res. Board, Nat. Res. Council.

Faheem, A., Cloutier, C., Bautista, E.G., Sobolev, K., 2017. Impact of coal combustion product incorporation in asphalt mixture performance. Transportation Research Board 96th Annual Meeting.

Faheem, A.F., Bahia, H.U., Faheem, A.F., Bahia, H.U., 2011. Modelling of asphalt mastic in terms of filler- bitumen interaction modelling of asphalt mastic in terms of filler-bitumen interaction. Road Mater. Pav. Design 0629 (sup1), 281–303.

FARCAS;, F., Mouillet;, V., Battaglia;, V., Besson;, S., Petiteau;, C., and Cunff, F. Le, 2009. Identification et dosage par spectrométrie infrarouge à transformée de Fourier des copolymères SBS et EVA dans les liants bitumineux. *Méthode D'Essai 71*, (ME 71), 16P.

Farrar, Michael J., Turner, Thomas F., Planche, Jean-Pascal, Schabron, John F., Harnsberger, P. Michael, 2013. Evolution of the crossover modulus with oxidative aging method to estimate change in viscoelastic properties of asphalt binder with time and depth on the road. Transport. Res. Rec. J. Transport. Res. Board 2370 (1), 76–83.

Grenfell, J., Gabet, T., Porot, L., de la Roche, C., Dubois, V., Van den bergh, W., and Van de Ven, M., 2009. Development of a laboratory bituminous mixtures aging protocol. Adv. Test. Character. Bitum. Mater., 331–346.

Guo, M. and Tan, Y., 2021. Interaction between asphalt and mineral fillers and its correlation to mastics ' viscoelasticity.

Lamontagne, J., Dumas, P., Mouillet, V., Kister, J., 2001. Comparison by Fourier transform infrared (FTIR) spectroscopy of different aging techniques: Application to road bitumens. Fuel 80 (4), 483–488.

Le, H.T., Inozemtcev, Sergey, Korolev, Evgeniy, Grishina, Anna, 2020. The efficiency of sulfur modifier to neutralize toxic gases in sulfur-asphalt concrete technology. IOP Conf. Series: Mater. Sci. Eng. 869 (3), 032016. https://doi.org/10.1088/1757-899X/869/3/032016.

Li, F. and Yang, Y., 2021. Experimental investigation on the influence of interfacial effects of limestone and fly ash filler particles in asphalt binder on mastic aging behaviors: Construct. Build. Mater., 290 (0).

Lesueur, Didier, Elwardany, Michael, Planche, Jean-Pascal, Christensen, Don, King, Gayle, 2021. Impact of the asphalt binder rheological behavior on the value of the DTc parameter. Construct. Build. Mater. 293, 123464. https://doi.org/10.1016/j.conbuildmat.2021.123464.

Liu, Guoqiang, Yang, Tao, Li, Jing, Jia, Yanshun, Zhao, Yongli, Zhang, Jiupeng, 2018. Effects of aging on rheological properties of asphalt materials and asphalt-filler interaction ability. Constr. Build. Mater. 168, 501–511.

Muhammad, Junaid, Peng, Tianyi, Zhang, Weiguang, Cheng, Hanglin, Waqas, Haroon, Abdul, Samad, Chen, Kunwei, Zhou, Yang, 2021. Moisture susceptibility and fatigue performance of asphalt binder modified by bone glue and coal fly ash. Constr. Build. Mater. 308, 125135. https://doi.org/10.1016/j.conbuildmat.2021.125135.

Nayak, Pratik, Sahoo, Umesh C., 2017. Rheological, chemical, and thermal investigations on an aged binder rejuvenated with two non-edible oils. Road Mater. Pav. Design 18 (3), 612–629.

Parvez, M.A., Al-mehthel, M., Wahhab, H.I.A., Hussein, I.A., 2014. Utilization of sulfur and crumb rubber in asphalt modification. J. Appl. Polym. Sci. 40046, 1–11.

Polacco, G., Filippi, S., Merusi, F., and Stastna, G., 2015. Historical perspective A review of the fundamentals of polymer-Modi fi ed asphalts : Asphalt/polymer interactions and principles of compatibility. *Advances in Colloid and Interface Science*, 224, 72–112.

Rahbar-Rastegar, R., 2017. Cracking in Asphalt Pavements : Impact Of Component Properties And Aging On Fatigue And Thermal. University of New Hampshire, Durham.

Rigden, P.J., 1947. The use of fillers in bituminous road surfacings. A study of filler-binder systems in relation to filler characteristics.pdf. Journal of the Society of Chemical Industry 66 (9), 299–309.

Saha, R., Malloy, K., Bautista, E., Sobolev, K., 2017. The investigation of fly ash based asphalt binders using atomic force microscope. *Higher Education Press and Springer-Verlag Berlin Heidelberg 2017*, 72 (1866), p.316.

Singh, B., Saboo, N., Kumar, P., 2017. Use of Fourier transform infrared spectroscopy to study aging characteristics of asphalt binders. Pet. Sci. Technol. 35 (16), 1648–1654.

Singh, M., Jain, K., Kahlon, S.S., 2020. Use of Sulphur as an Additive in Bitumen : A Review. Internat. Res. J. Eng. Technol. (IRJET) 07 (10), 36–43.

Sinsiri, Theerawat, Chindaprasirt, Prinya, Jaturapitakkul, Chai, 2010. Influence of fly ash fineness and shape on the porosity and permeability of blended cement pastes. Int. J. Miner. Metall. Mater. 17 (6), 683–690.

Sobolev, K., Vivian, I.F., and Faheem, A., 2014. Application of Fly Ash in ASHphalt Concrete : from Challenges to Opportunities Application of Fly Ash in ASHphalt Concrete : from Challenges to Opportunities. *World of Coal Ash Conference*, (May).

Smith, Benjamin James, 2001. Low-temperature and dynamic fatigue toughening mechanisms in asphalt mastics and mixtures. Postgraduate Dissertation, Queen's University, Kingston, Canada.

Wang, C., Castorena, C., Zhang, J., Kim, Y.R., Wang, C., Castorena, C., Zhang, J., Unified, Y.R.K., 2015. Unified failure criterion for asphalt binder under cyclic fatigue loading. Road Mater. Pav. Design 0629 (16:sup2), 125–148.

Wu, Shaopeng, Pang, Ling, Liu, Gang, Zhu, Jiqing, 2010. Laboratory study on ultraviolet radiation aging of bitumen. J. Mater. Civ. Eng. 22 (8), 767–772.

Xie, Wei, Castorena, Cassie, Wang, Chao, Richard Kim, Y., 2017. A framework to characterize the healing potential of asphalt binder using the linear amplitude sweep test. Construct. Build. Mater. 154, 771–779.

Xu, Xiong, Yu, Jianying, Xue, Lihui, Zhang, Canlin, Zha, Yagang, Gu, Yi, 2017. Investigation of molecular structure and thermal properties of thermo-oxidative aged SBS in blends and their relations. Materials 10 (7), 768. https://doi.org/10.3390/ma10070768.

Yang, X., You, Z., Ph, D., Asce, M., Mills-Beale, J., 2015. Asphalt binders blended with a high percentage of biobinders : Aging mechanism using FTIR and rheology. J. Mater. Civ. Eng. 27 (4), 1–11.

Yu, Huanan, Bai, Xianping, Qian, Guoping, Wei, Hui, Gong, Xiangbing, Jin, Jiao, Li, Zhijie, 2019. Impact of ultraviolet radiation on the aging properties of SBS-modified asphalt binders. Polymers 11 (7), 1111. https://doi.org/10.3390/polym11071111.

Zhang, J., Li, X., Liu, G., Pei, J., 2019. Effects of material characteristics on asphalt and filler interaction ability. Int. J. Pavement Eng. 8436, 1–10.